VOL. X, NO. X, XXXXXXXX ISSN 1819-6608
ARPN Journal of Engineering and Applied Sciences

www.arpnjournals.com

LOW COST AND ROBUST ROTOR THREE-PHASE WOUND-FIELD SWITCHED-FLUX MACHINES FOR HEV APPLICATIONS

Faisal Khan, Erwan Sulaiman, Mohd Fairoz Omar,
Hassan Ali Soomro
Research Center for Applied Electromagnetics, Universiti Tun Hussein Onn Malaysia, 86400, Johor, Malaysia
E-Mail: faisalkhan@ciit.net.pk

ABSTRACT
Wound-field switched-flux machines (WFSFM) have an intrinsic simplicity and high speed that make them well suited to many hybrid electric vehicle (HEV) applications. However, overlap armature and field windings raised the copper losses in these machines. Furthermore, segmented-rotor configuration is employed to enhance the characteristics of motor, however it made the rotor less robust and cannot be applied in high speed applications. To overcome these problems, this paper presents novel topologies for three-phase wound-field switched-flux machines. Both armature and field winding are located on the stator and rotor is composed of only stack of iron. Non-overlap windings and salient rotor are the clear advantages of these topologies as the copper losses gets reduce and rotor becomes more robust. Design feasibility and performance analysis of 12 slots and different rotor pole numbers are examined on the basis of coil arrangement test, peak armature flux linkage, back emf and cogging torque by using Finite Element Analysis (FEA). Flux distributions, split ratio and average torque are also investigated for 12Slot-8Pole and 12Slot-7Pole WFSFM.

Key words: Electric motors · Hybrid electric vehicles · rotor · stator · torque measurement ·

INTRODUCTION

Global warming is the increase in the mean surface temperature of the earth and has become an important issue in the 21st century. Scientists reported that various causes for global warming include the geomagnetic variation, the variations in the incoming solar radiation (Goode and Palle, 2007), and the increasing concentration of greenhouse gases by certain human activities such as burning of fossil fuels, deforestation etc (Samuel and Sivamadhavi, 2010). The conventional internal combustion engine (ICE) vehicles are also the main contributors on this issue. In response to global warming issue, HEV's were the proposed solution to reduce the concentration of greenhouse gases. HEV has two power sources: one bidirectional power source based on electrical energy storage subsystem with an electric machine and the other unidirectional power source based on ICE (Gao and Ehsani, 2006), (Ehsani, Gao, and Miller, 2007).

Any electric machine, DC or AC, is considered as a physical device to accomplish electromechanical energy conversion. Electrical motor that transforms the electrical energy to mechanical energy is categorized into two main classes that are direct current (DC) motor and alternating current (AC) motor and then further classified as shown in Figure 1. The basic requirements of an electric machine for electric vehicle drive system are high efficiency; high torque density and constant power at high speed (Xu et al., 2009), (Fan et al., 2014). Switched-flux motor (SFM), a new class of electric motor having high torque and power density is used in HEV which is the combination of the switched reluctance motor and an inductor alternator (Walker, 1942), (Miller, 1993). SFM can be classified into three groups that are permanent magnet SFM, field excitation SFM and hybrid excitation SFM. The main source of flux in permanent magnet SFM is permanent magnet and field excitation coil (FEC) in field excitation SFM while both permanent magnet and FEC in hybrid excitation SFM (Zhu, 2011), (Sulaiman, Kosaka, and Matsui, 2011), (Sulaiman, Kosaka, Matsui, 2014). Armature winding and field winding or permanent magnet are located on the stator in these SFMs. The field excitation SFM has advantages of low cost, simple construction, magnet-less machine, and variable flux control capabilities suitable for various performances when compare with others SFMs. Due to these advantages, a 24S-10P three-phase WFSFM has been developed from 24S-10P permanent magnet SFM in which the permanent magnet is replaced by FEC as shown in Figure 2(a) (Chen et al., 2010). The total flux generation is limited because of adjacent DC FEC isolation and thus machine performance is affected. To overcome the drawbacks, a new structure of 24S-10P and 24S-14P field excitation SFM with single DC polarity have been introduced and compared as depicted in Figure 2(b)

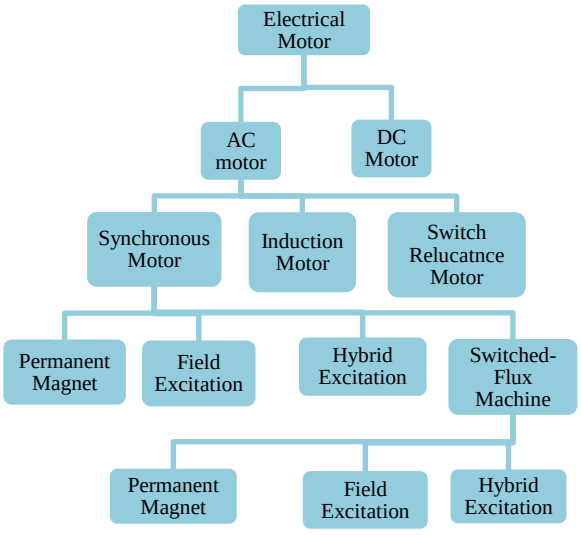

Figure 1: Classification of Electrical Motors

(Sulaiman et al., 2013). Although less leakage flux and uncomplicated manufacturing of single DC FEC are the advantages of proposed machine but it has overlapping armature and field winding which increases the cost, copper losses and thus reduce the efficiency. The performance of SFM is enhanced by using segmental rotor configuration in recent research (Mecrow et al., 2003). Segmental rotor is designed in a manner such that to achieve bipolar flux in armature winding, which has neither magnets nor winding. To produce bipolar flux linkages in this way, a toothed-rotor structure may be used but it requires overlap windings on the stator (Sulaiman, Kosaka and Matsui, 2012). The configuration of concentrated windings or non-overlap winding, instead of distributed windings or overlap winding, is used nowadays because of its advantages of short end windings and simple structure. If the slot pitch is close to the pole pitch as in case of similar numbers of slots and poles, then copper losses get reduced and high torque is produced in non-overlap winding, discussed in (Ishak, Zhu and Howe, 2006), (Hwang, Cheng, and Chang, 2005). Non-overlap winding has been used in (Zulu, Mecrow and Armstrong, 2010) to increase the efficiency by reducing the copper losses and enhanced the speed torque characteristics of SFM. A three-phase SFM using a segmental rotor has been proposed in (Zulu, Mecrow, and Armstrong, 2010) to improve fault tolerance to a reduction in torque pulsations and power converter rating per phase. Figure 2(c) (Sulaiman, Kosaka and Matsui, 2012) and Figure 2(d) (Zulu, Mecrow, and Armstrong, 2010) show SFMs having toothed-rotor with overlap windings and segmented-rotor with non-overlap windings at the stator. A single-phase WFSFM machine was comprehensively investigated in (Pollock, Pollock, and Brackley, 2003), (Pollock et al. 2006). In that machine, armature and field windings are fully pitched and hence the end-winding is long. Two single phase WFSFMs topologies with DC field and AC armature windings having the same coil-pitch of 2 slot-pitches and having different coil-pitches of 1 and 3 slot-pitches respectively are discussed (Zho and Zhu, 2013). It is shown that the iron loss and copper loss of WFSFM has been reduced and thus increased the efficiency.

This paper explains the feasible topologies for three-phase WFSFM having toothed-rotor structure and non-overlap armature and field winding. Design feasibility and performance analysis of 12 slots (6 slots for FEC and 6 slots for armature coil) and different rotor pole numbers are examined on the basis of coil arrangement test, peak armature flux linkage, back emf and cogging torque. Two WFSFMs topologies, 12Slot-8Pole and 12Slot-7Pole are compared and analyzed in terms of their average torque and torque versus power, speed characteristics. FEA simulations, conducted via JMAG-Designer ver. 13.0 released by Japan Research Institute (JRI) are used to study various characteristics of design.

OPERATING PRINCIPLE OF WFSFM

The term "flux switching" is introduced by changing the polarity of flux linkage, following the motion of salient pole rotor. FEC and armature coil are the main sources of flux for WFSFM and both the sources are located on the stator. When the armature and FEC are energized, the rotor arranges itself into a position of minimum reluctance with the stator and hence torque is produced. Figure 3 demonstrate the operating principle of WFSFM where the flux generated by FEC and armature coil flow from stator into rotor and from rotor into stator to produce a complete flux cycle. The direction of current flow in winding is denoted by conventional dot and cross. When the rotor moves to the right, the rotor pole goes to the next stator tooth, hence switched the magnitude and polarities of the flux linkage. The flux does not rotate but shifts clockwise and counterclockwise direction with each armature current reversal. The possible number of rotor pole and stator slot is defined by,

$$N_{rotor} = N_{stator}\left(1 \pm \frac{k}{2q}\right) \quad (1)$$

where k is natural entity from 1 to 5, q is number of phases having value 3, N_{rotor} is the number of rotor poles and N_{stator} is the number of stator slots having value 6 in the proposed WFSFM.

VARIOUS TOPOLOGIES FOR THE PROPOSED WFSFM

A three-phase SFM is proposed using 12 stator teeth and various rotor pole of 5, 7, 8, 10, 11, as shown in Figure 4 while design specifications are illustrated in Table 1. In all topologies, six of the 12 stator teeth, denoted as FEC1 to FEC6, are wound as field coil and excited with dc while the remaining six teeth contain six armature coils, U1,U2,V1,V2,W1 and W2 which make two sets of three-phase winding. Both the FEC and armature winding are placed in the stator which didn't overlap each other. The width of stator tooth is made equal to width of rotor tooth, to allow the flux to flow easily and avoid saturation at stator core. As the salient rotor rotates, the WFSFM involves changing the polarity of the DC field excitation flux linking with the armature coil flux and this is the basic mechanism of flux switching.

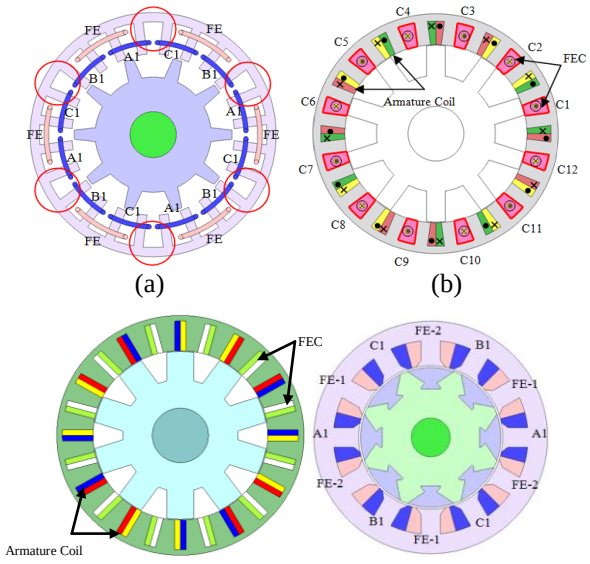

Figure 2: (a)Three-phase 24S-10P field excitation SFM, (b) 24S-10P single DC WFSFM, (c) Toothed-rotor three-phase WFSFM, (d) Segmented-rotor three-phase WFSFM

COIL ARRANGEMENT TEST OF THREE-PHASE WFSFM

Coil arrangement test are normally performed to confirm the operating principle of three-phase WFSFM and to set the position of each armature coil phase. The FECs are wounded in alternate direction as illustrated in Figure 4. Field winding is excited by applying 390.34A current and flux linkage at each coil is observed. By comparing the flux linkages of different coils, the armature coil phases have 120^0 phase shift. The three-phase flux linkage waveforms, defined as U, V, and W is observed. The same procedures are applied for all slot-rotor pole arrangements to confirm the operating principle and three phase flux linkages of WFSFM. From Figure 5, it is obvious that 12Slot-5Pole has high flux linkage as compare to other WFSFM topologies. This means that the 12Slot-5Pole configuration has possibility to provide higher torque and power but this topology is not practical due to unbalanced magnetic force. For the rest of rotor pole numbers, the less amplitude of flux linkage is due to some flux leakage occurs when higher rotor pole number is used in the design and will further investigate in future. Thus, the coil tests to proof the principle of operation and to get three phase flux linkages of the WFSFMs are successfully achieved.

BACK EMF AND COGGING TORQUE ANALYSIS OF WFSFMS

At no load such that armature current, I_a of 0A, the induced voltage generated from FEC with the speed of 1200 r/min for different rotor pole numbers are illustrated in Figure 6. It is noticed that 12Slot-10Pole has highest amplitude back emf of approximately 33V, followed by 12Slot-5Pole which has approximately 31V while 12Slot-

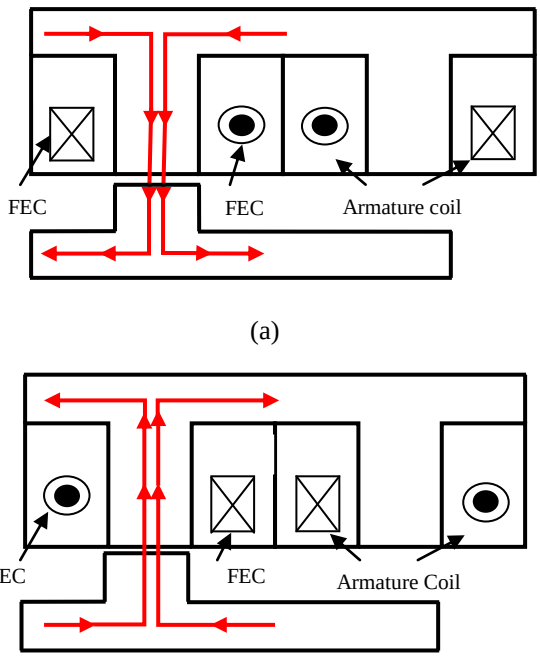

Figure 3: Principle of operation of WFSFM (a) flux flows from stator to rotor (b) flux flows from rotor to stator

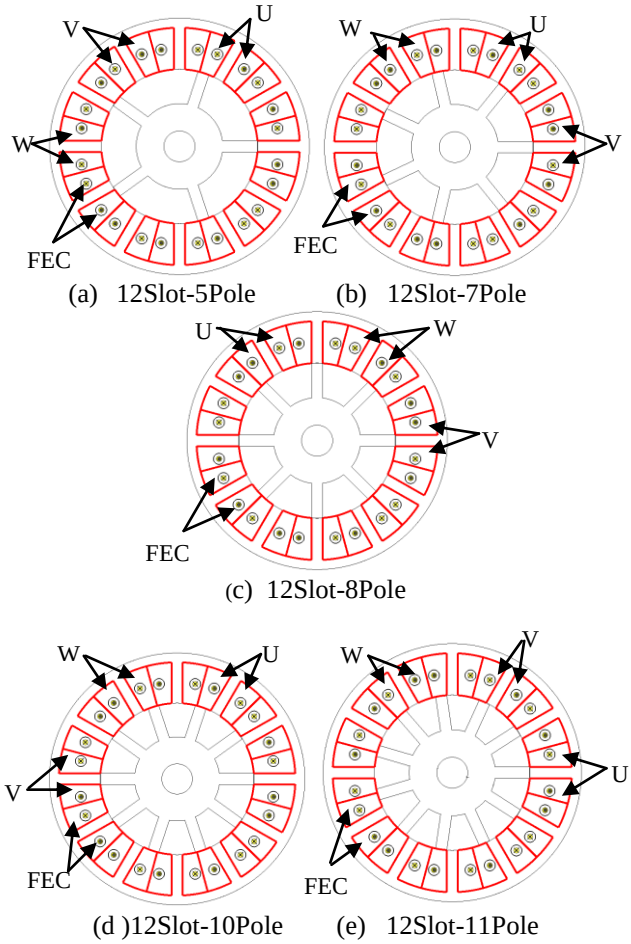

Figure 4: Three-phase WFSFM topologies having different rotor pole number

Table 1. Three-phase WFSFM design specifications

Parameters	Values
Rated speed	1200 rev/min
Stator slot number	12
Air-gap length	0.3mm
Diameter of rotor	180mm
Outside diameter of stator	300mm
Width of stator tooth	13mm
Back iron depth of stator	11mm
Motor stack length	80mm
Number of turns per FE Coil slot	44
Number of turns per armature coil slot	44
Total armature slot area	1145.017mm^2
Total field slot area	1145.017mm^2
Filling factor	0.5

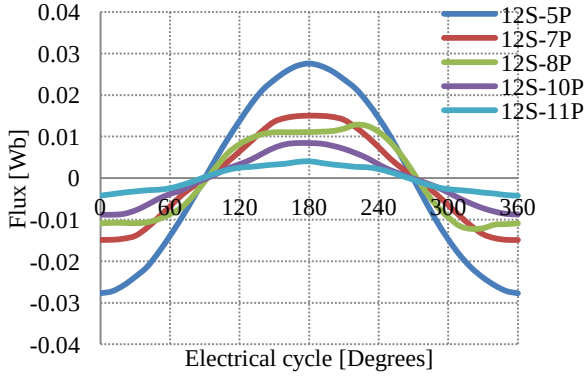

Figure 5: U-phase flux linkages of all WFSFMs

11Pole has the least back emf amplitude of 10V and the waveform is distorted due to 3rd and 7th harmonics. Back emf at no load condition of all topologies is less than applied voltage which makes it easy to provide protection when the inverter is in off state due to some faults. The cogging torque analysis for different pole numbers are examined by setting armature current density, J_a of 0 A_{rms}/mm^2 and field current density, J_e at maximum value of 30 A/mm^2. Figure 7 shows the cogging torque characteristics of various topologies. 12Slot-10Pole WFSFM topology has highest peak to peak cogging torque of approximately 50Nm while 12Slot-7Pole has least peak to peak cogging torque which is about 3Nm. As high cogging torque causes vibration in machine and makes it noisy, therefore by further design refinement and optimization, the cogging torque can be reduced to an acceptable condition.

FLUX CHARACTERISTICS AT VARIOUS FIELD CURRENT DENSITY, J_E AND FLUX DISTRIBUTION

Two WFSFM topologies 12Slot-8Pole and 12Slot-7Pole are chosen to examine their flux characteristics due to less cogging torque and high flux linkage. The flux characteristics for 12Slot-8Pole and 12Slot-7Pole at various DC FEC current densities, J_e are illustrated in Figure 8. It is obvious from both figures that flux pattern increase linearly by increasing field current density, J_e. From Figure 9, it is noticeable that 12Slot-7Pole has maximum flux density of 2.93 T and 12Slot-8Pole has value of 2.53 T. The pole tip of 12Slot-8Pole is saturated as indicated by red circles. The saturation effect will be removed by changing various

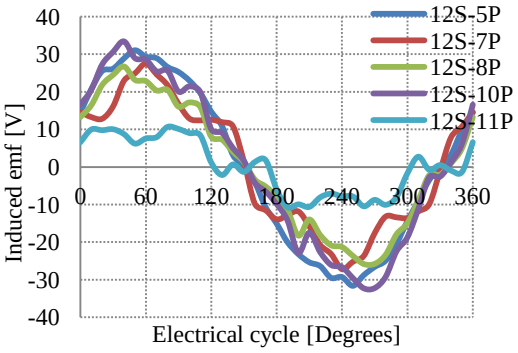

Figure 6: Back emf waveform of WFSFM at 1200 rpm

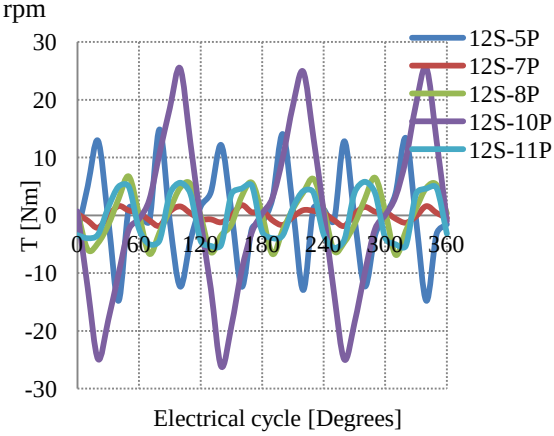

Figure 7: Cogging Torque

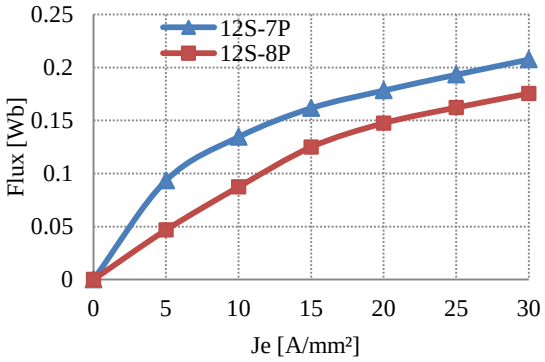

Figure 8: Comparisons of flux vs. J_e for WFSFMs

design parameters. Both designs have high flux leakage from the core to surrounding area as illustrated in Figure 9 but it can be minimized by design refinement.

SPLIT RATIO

The split ratio defined as, rotor outer diameter/stator outer diameter of WFSFM is a key design parameter. When the copper losses are fixed, the optimized split ratio is not sensitive to number of rotor poles (Amara et al., 2005), (Chen and Zhu, 2009). The variation of torque with split ratio is shown in Figure 10. Both designs have maximum average torque at split ratio of 0.7. The average torque at 0.4 split ratio is approximately 3 times less than torque at 0.7 because the diameter of rotor has less value as compared

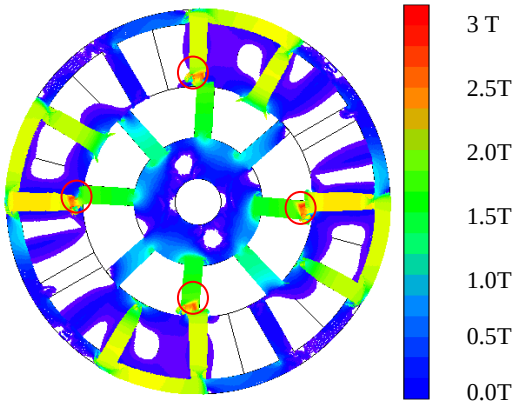

(a) 12Slot-8Pole

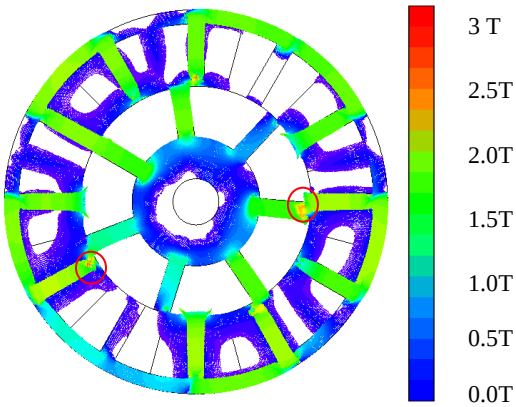

(b) 12Slot-7Pole

Figure 9: Flux distribution of WFSFMs

with other designs.

TORQUE VS. ARMATURE CURRENT DENSITY AND FIELD CURRENT DENSITY CURVES

The torque vs. armature current density, J_a curves for various field current density, J_e is shown in Figure 11 and Figure 12. Form both graphs, the same pattern of linear increment of torque with respect to increase in J_e and J_a is observed. At low field current density, J_e of 5A/mm^2, the torque of 12Slot-8Pole is increased to 32Nm until armature coil current density, J_a of 20Arms/mm^2 and then decreased when armature current density is further increased. This is due to low field coil flux that limits the force to move the rotor. The torque of 12Slot-8Pole is 60Nm at J_e of 15 A/mm^2 almost double to 12Slot-7Pole which is approximately 31Nm. Therefore, a good balance between field coil and armature coil current densities should be determined to get the required torque at specific condition while minimizing the copper loss. From the comparison of both figures, it is obvious that 12Slot-8Pole design has high torque values.

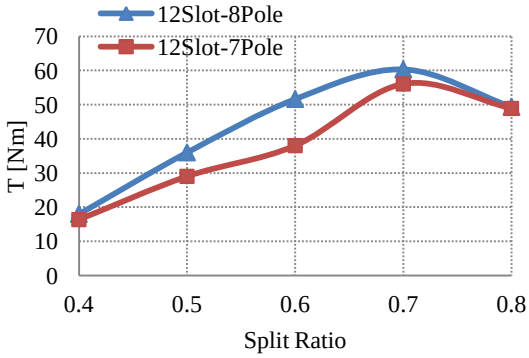

Figure 10: Influence of split ratio on 12Slot-8Pole and 12Slot-7Pole WFSFMs

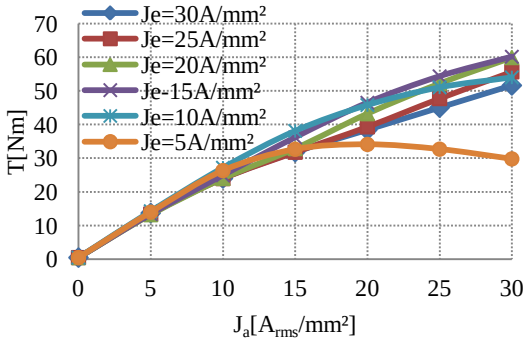

Figure 11: Torque Vs. J_a at various J_e for 12Slot-8Pole

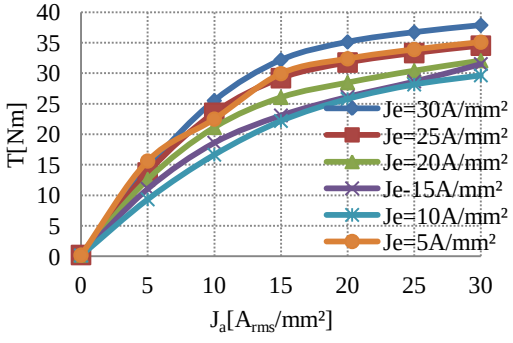

Figure 12: Torque Vs. J_a at various J_e for 12Slot-7Pole

TORQUE AND POWER VERSUS SPEED CHARACTERISTICS OF 12SLOT-8POLE AND 12SLOT-7POLE WFSFM

The torque and power versus speed curves of 12Slot-8Pole and 12Slot-7Pole WFSFMs are plotted in Figure 13. At the base speed of 2106.83 rev/min and 2308.36 rev/min, the maximum torque of 60.17 Nm and 38.45 Nm is obtained and torque starts to decrease if the machine is operated beyond the base speed. Moreover, both WFSFMs has high speed at light load condition and the speed reduces by increasing the load. Various speed control methods can be used in future to operate this motor at variable load conditions, as discussed in (Sudarsan et al., 2014). The power accomplished by 12Slot-8Pole WFSFM at maximum torque and base speed of 2106.83 rev/min is 12.79 kW and starts to reduce until 10kW at higher speed of 5802.7 rev/min due to increase in iron loss while the power achieved by 12Slot-7Pole WFSFM is 9.3kW at maximum torque and base speed of 2308.36 rev/min.

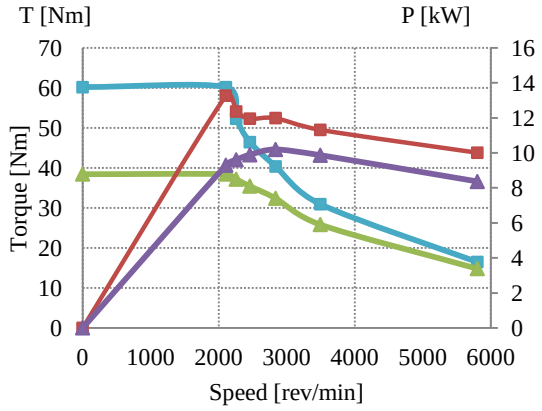

Figure 13: Torque Vs. power and speed characteristics for 12Slot-8Pole and 12Sot-7Pole WFSFMs

CONCLUSION

This paper demonstrates five topologies of three-phase salient rotor WFSFM with non-overlap armature and field windings. In comparison with permanent magnet AC machines, it has low cost due to no permanent magnet and the field flux can be easily controlled. Due to replacement of segmental rotor by salient rotor, the mechanical strength of the WFSFM is improved and becomes more suitable for high speed EV drive. Thus, it can be defined as simple configuration, low cost and high efficiency machine. Although 12Slot-7Pole has high flux linkage and least cogging torque but it is not practical due to unbalanced magnetic force. Topologies with an even number of rotor teeth may have immediate practical use. Therefore, 12Slot-8Pole WFSFM can be considered as the best machine because it has achieved better performances based on FEA and can be further improved in future in terms of cogging torque and flux linkage by design refinement and optimization.

REFERENCE

Amara, Y., Hoang, E., Gabsi, M., Lecrivain, M. and Allano, S. (2005). Design and comparison of different flux-switch synchronous machines for anaircraft oil breather application. *Eur. Trans. Elect. Power*, 15(6), pp. 497-511.

Chen, J. T., Zhu, Z. Q., Iwasaki, S. and Deodhar, R. (2010). Low cost flux-switching brushless AC machines. *Proc.IEEE Vehicle Power and Propulsion Conf*., Lille, France, pp.1-6.

Chen, J. T. and Zhu, Z. Q. (2009). Parameter optimization of flux-switching PM brushless ac machines having alternative stator and rotor pole numbers. in *Proc. IEEE Int. Electric Mach. Drives Conf.*, pp. 1451-1458.

Ehsani, M., Gao, Y. and Miller, J. M. (2007), Hybrid electric vehicles: Architecture and motor drives. *Proc. IEEE*, 95(4), pp. 719-728.

Fan, Y., Gu L., Luo, Y., Han, X. and Cheng, M. (2014). Investigation of a New Flux-Modulated Permanent Magnet Brushless Motor for EVs, *The Scientific World Journal*, (2014), pp.1-9.

Gao ,Y. and Ehsani, M. (2006). A torque and speed coupling hybrid drive train- architecture, control, and simulation. *IEEE Trans. Power Electron.*, 21(3), pp. 741-748.

Goode, P.R. and Palle, E. (2007). Shortwave forcing of the Earth's climate: Modern and historical variations in the Sun's irradiance and the Earth's reflectance. *J Atmos Sol-Terr Phy*, 69, pp. 1556-1568.

Hwang, C. C., Cheng, S. P. and Chang, C. M. (2005). Design of high-performance spindle motors with concentrated windings. *IEEE Transactions on Magnetics*, 41, pp.971-973.

Ishak, D., Zhu, Z. Q. and Howe, D. (2006). Comparison of PM brushless motors, having either all teeth or alternate teeth wound. *IEEE Transactions on Energy Conversion*, 21, pp. 95-103.

Mecrow, B.C., El-Kharashi, E.A., Finch, J.W. and Jack, A.G. (2003). Segmental rotor switched reluctance motors with single-tooth windings. *IEE Proc. on Power Applications*, 150(5), pp. 591-599.

Miller, T. J. E. (1993). Switched Reluctance Machines and Their Control, Hillsboro, OH: Magna Physics.

Pollock, C., Pollock, H. and Brackley, M. (2003). Electronically controlled flux switching motors: A comparison with an induction motor driving an axial fan. *in Conf. Rec. IEEE IAS Annu. Meeting*, pp. 2465-2470.

Pollock, C., Pollock, H., Barron, R., Coles, J. R., Moule, D., Court, A. and Sutton, R. (2006). Flux-switching motors for automotive applications. *IEEE Trans. Ind. Appl.*, 42(5), pp 1177-1184.

Samuel S. R. and Sivamadhavi, V. (2010). Magnitude of Green House Effect and the Contribution of Carbon Di Oxide. *Recent Advances in Space Technology Services and Climate Change (RSTSCC)*, pp.41- 44.

Sudarsan, B. S., Kumar, M. S., Ramasamy, S.and Ramanathan, P. (2014). Design and Implemenation of Fuzzy Logic control based speed control of industrial conveyor. *ARPN Journal of Engineering and Applied Sciences*, 9(9), pp. 1547-155

Sulaiman, E., Kosaka, T. and Matsui N. (2011). A new structure of 12Slot-10Pole field-excitation flux switching synchronous machine for hybrid electric vehicles. *IEEE, 14th European Conference on Power Electronics and Applications*, pp. 1-10.

Sulaiman E., Kosaka T., Matsui N. (2014). Design and analysis of high-power/high-torque density dual excitation switched-flux machine for traction drive in HEVs. *Renewable and Sustainable Energy Review*, 34, pp. 517-524.

Sulaiman, E., Teridi, M. F., Husin, M. Z. A., Ahmad M. Z. and Kosaka, T. (2013). Performance Comparison of 24S-10P and 24S-14P Field Excitation Flux Switching Machine with Single DC-Coil Polarity. *Proc. on Int. Power Eng. & Optimization Conf*., pp. 46-51.

Sulaiman, E., Kosaka T. and Matsui N. (2012). Design Study and Experimental Analysis of Wound Field FluxSwitching Motor for HEV Applications. *2012 XXth International Conference on Electrical Machines (ICEM*), pp. 1269 -1275.

Walker, J. H. (1942). The theory of the inductor alternator. *J. IEE*, 89(9),pp.227-241.

Xu, W., Zhu, J., Guo, Y., Wang, S., Wang, Y. and Shi, Z. (2009). Survey on electrical machines in electrical vehicles. *International Conference on Applied Superconductivity and Electromagnetic Devices*, pp. 167-170.

Zhu, Z. Q. (2011). Switched flux permanent magnet machines: Innovation continues. in Proc. Int. Conf. on Electrical Machines and Systems (ICEMS), pp.1-10.

Zho, Y. J. and Zhu Z. Q. (2013). Comparison of low-cost single-phase wound-field switched-flux machines. *Electric Machines & Drives Conference (IEMDC)*, pp. 1275-1282.

Zulu, A., Mecrow, B.C. and Armstrong, M. (2010). Topologies for three-phase Wound field Segmented-Rotor flux switching Machines. *5th IET International Conference on Power Electronics, Machines and Drives*, pp.1-6.

Zulu, A., Mecrow, B. C. and Armstrong M. (2010). A Wound-Field Three-Phase Flux-Switching Synchronous Motor with all Excitation Sources on the Stator. *IEEE Transactions on Industry Applications*, 46(6), pp.2363-2371.